ARTICLE

Magnetic resonance texture analysis reveals stagewise nonlinear alterations of the frontal gray matter in patients with early psychosis

Sun Young Moon[1,2], Hyungyou Park[3], Won Lee[3], Subin Lee[3], Silvia Kyungjin Lho[4], Minah Kim[5,6], Ki Woong Kim[2,3,6,7] and Jun Soo Kwon[2,3,5,6]✉

Although gray matter (GM) abnormalities are present from the early stages of psychosis, subtle/miniscule changes may not be detected by conventional volumetry. Texture analysis (TA), which permits quantification of the complex interrelationship between contrasts at the individual voxel level, may capture subtle GM changes with more sensitivity than does volume or cortical thickness (CTh). We performed three-dimensional TA in nine GM regions of interest (ROIs) using T1 magnetic resonance images from 101 patients with first-episode psychosis (FEP), 85 patients at clinical high risk (CHR) for psychosis, and 147 controls. Via principal component analysis, three features of gray-level cooccurrence matrix – informational measure of correlation 1 (IMC1), autocorrelation (AC), and inverse difference (ID) – were selected to analyze cortical texture in the ROIs that showed a significant change in volume or CTh in the study groups. Significant reductions in GM volume and CTh of various frontotemporal regions were found in the FEP compared with the controls. Increased frontal AC was found in the FEP group compared to the controls after adjusting for volume and CTh changes. While volume and CTh were preserved in the CHR group, a stagewise nonlinear increase in frontal IMC1 was found, which exceeded both the controls and FEP group. Increased frontal IMC1 was also associated with a lesser severity of attenuated positive symptoms in the CHR group, while neither volume nor CTh was. The results of the current study suggest that frontal IMC1 may reflect subtle, dynamic GM changes and the symptomatology of the CHR stage with greater sensitivity, even in the absence of gross GM abnormalities. Some structural mechanisms that may contribute to texture changes (e.g., macrostructural cortical lamina, neuropil/myelination, cortical reorganization) and their possible implications are explored and discussed. Texture may be a useful tool to investigate subtle and dynamic GM abnormalities, especially during the CHR period.

Molecular Psychiatry; https://doi.org/10.1038/s41380-023-02163-3

INTRODUCTION

Gray matter (GM) abnormalities are an established finding in patients with schizophrenia. Decreases in regional gray matter volumes (GMVs) and cortical thickness (CTh) are consistently reported [1–3] and are acknowledged to be present from even first-episode psychosis (FEP) [4, 5]. While the degree of GM reductions is greater in the chronic stage [3, 6], the rate of change is thought to be greatest during the early stages [2, 6], with frontotemporal regions being the most affected [2].

Clinical high risk (CHR) for psychosis, also referred to as the at-risk mental state, constitutes a critical period in the early prevention strategies for schizophrenia. However, unlike patients with schizophrenia or FEP, there are mixed results regarding the findings of GM abnormalities in CHR individuals. While some studies reported a lesser degree of GMV or CTh decrease mainly in the frontal regions [7–10], other studies, including a recent meta-analysis, demonstrated either an equivocal finding [11] or even an increase in GMV [10, 12]. Even in studies that reported GMV or CTh reductions in the CHR period, the regions appeared to be more varied, with inconsistent reports of association with symptoms [10, 12–14] relative to the results of FEP studies. While both the more heterogeneous nature of CHR subjects and the tendency toward less prominent GM alterations are thought to underlie discrepancies in GM findings, measurements that are more sensitive to subtle GM changes than conventional volume- or CTh-based metrics may prove more useful in investigating subtle/miniscule GM abnormalities in the CHR period.

Meanwhile, texture analysis (TA) performs a quantitative analysis of the mainly qualitative attributes of an image by analyzing locally complex interrelationships of voxel contrasts. The strengths of TA lie in its ability to measure complex or subtle changes occurring at an individual voxel level, which can capture minuscule changes not otherwise detectable by volumetric or signal intensity measures [15]. TA has been applied to various

[1]Department of Public Health Service, Seoul National University Bundang Hospital, Seongnam, Republic of Korea. [2]Institute of Human Behavioral Medicine, Seoul National University Medical Research Center, Seoul, Republic of Korea. [3]Department of Brain and Cognitive Science, Seoul National University College of Natural Science, Seoul, Republic of Korea. [4]Research and Development Division, 40FY Inc., Seongnam, Republic of Korea. [5]Department of Neuropsychiatry, Seoul National University Hospital, Seoul, Republic of Korea. [6]Department of Psychiatry, Seoul National University College of Medicine, Seoul, Republic of Korea. [7]Department of Neuropsychiatry, Seoul National University Bundang Hospital, Seongnam, Republic of Korea. ✉email: kwonjs@snu.ac.kr

Received: 15 December 2022 Revised: 13 June 2023 Accepted: 23 June 2023
Published online: 27 July 2023

imaging modalities in medical research, most actively in the fields of oncology to aid in diagnoses, quantify lesion properties, or predict prognoses [16, 17]. It has also shown promising results for its application in various central nervous system disorders [15, 18–22]. These results indicate that TA can have greater sensitivity and add complementary clinical information than conventional measures of volume [15, 22], with particular strengths for early diagnosis and monitoring of disease states [23].

However, the scope of current texture research in schizophrenia is constrained by limited sample sizes, a tendency to focus on the chronic stage, and diverse methodologies for texture extraction [24–26]. Furthermore, these studies have overlooked the possibility of examining the cortical GM in a systemic manner; instead, they have chosen to focus on unsegmented whole-brain images [24, 25, 27, 28] or a singular region of interest (ROI) [29]. Notably, a recent study by Korda et al. [28] used whole-brain texture to categorize FEP and CHR subjects via explainable artificial intelligence, a significant step forward. However, this approach may not fully capture the subtle and spatially heterogeneous GM changes that occur during the early stages of psychosis [2, 6, 30], since attributing whole-brain texture changes to specific GM abnormalities can present a challenge due to the spatial and volumetric compression of GM compared to white matter and ventricular spaces. Our study aims to fill this gap by focusing on GM ROIs implicated in early-stage psychosis. More specifically, given the sensitivity of texture measures to microstructural abnormalities [15, 22, 31] and the nature of the established [4, 5] yet spatially uneven GM changes [1, 2, 6, 30] during these early stages, we posit that conducting a granular investigation of individual GM ROIs using TA could provide additional useful insights into the dynamic GM changes that occur during these crucial stages. This more detailed, ROI-focused methodology stands in contrast to existing practices [24–29] and may enable a more refined understanding of the subtle, dynamic GM changes that unfold during the early stages of psychosis, as compared to relying solely on measures such as volume, CTh, or unsegmented whole-brain images.

Thus, this study investigated GM texture changes in FEP and CHR patients compared to healthy controls (HCs). We first identified the regions in FEP and CHR patients that showed significant abnormalities in terms of volume, CTh, or surface area (SA) when compared to HCs and performed TA on those regions. We excluded the regions without any significant group effect from the TA step because those regions were less likely to be affected by early-stage psychosis as a whole, which, if included, could confound later interpretations of texture group effects. We hypothesized that (1) concurrent with previous studies, regional GM abnormalities (in terms of the combination of volume, CTh, SA, texture) would be observed in the FEP group, while in the CHR group, such changes may or may not be present, (2) different texture features may show associations with different measures of GM structure (GMV, CTh, SA), and (3) TA may more sensitively capture GM changes during the early phases of psychotic illness; it may also hold additional information than conventional volume- or CTh-based measures.

METHODS

Study participants and clinical assessments

A total of 101 patients with FEP, 85 individuals at CHR for psychosis, and 147 HCs were included. FEP and CHR individuals were recruited from the prospective, longitudinal cohort study conducted at the Seoul Youth Clinic (http://www.youthclinic.org) in Seoul National University Hospital (SNUH) [32]. FEP was defined as meeting the criteria for either schizophreniform, schizophrenia, or schizoaffective disorder as described in the Structured Clinical Interview for DSM-IV Axis I disorders (SCID-I), with the duration of illness being less than 2 years. The Positive and Negative Symptom Scale (PANSS) [33] was used to assess the symptom severity of FEP participants. CHR status was screened and confirmed by psychiatric specialists using the Structured Interview for Prodromal Symptoms (SIPS) [34]. The symptom severity of CHR participants was assessed using the Scale of Prodromal Symptoms (SOPS). Since antipsychotic medication had the potential to confound study findings, four CHR participants who were taking antipsychotic medication at their baseline assessment were excluded. Participants in the control group without any family history of psychiatric disorders were recruited using internet advertisements; they were screened for Axis I disorders using SCID-I Non-Patient Edition (SCID-NP) [35]. Individuals with any current/past psychiatric illness were excluded from the HC group. Common exclusion criteria for all the participants included (1) intellectual disability defined as an intellectual quotient less than 70, (2) substance use disorder, (3) history of head trauma with loss of consciousness, (4) history of seizure, and (5) presence or history of any significant medical/surgical illnesses.

All study participants were given a thorough explanation of the study, willingly agreed to participate, and provided written informed consent (IRB no. H-1110-009-380, H-1511-069-719). This study was conducted in accordance with the Declaration of Helsinki and was approved by the Institutional Review Board of SNUH (IRB no. H-2108-245-1252).

Magnetic resonance imaging (MRI) acquisition and processing

We acquired T1-weighted MRI data using a Siemens 3T Magnetom Trio Tim syngo MR scanner and implemented a 3D MPRAGE sequence. Key parameters included a repetition time of 1670ms, echo time of 1.89 ms, and voxel size of $1 \times 0.98 \times 0.98\ mm^3$. Post-acquisition, all T1 images underwent visual inspection for artifacts/lesions. Further processing and segmentation were conducted via FreeSurfer (version 6.0), with automated processes for motion correction, non-brain tissue removal, and Talairach transformation. Subsequent ROI segmentation, regional GMV, total intracranial volumes (ICV), CTh, and SA measurements were also obtained. We excluded the hippocampus from CTh due to its folded structure with bulbous characteristics compared to the thin, ribbon-like appearance of other cortical GMs, which makes it more difficult to reliably calculate the thickness values [36]. Additional procedural details are available in the Supplementary Information.

Selection of regions of interest (ROI)

We searched relevant review articles or meta-analyses to select the most relevant ROIs (Supplementary Table 1, Supplementary Fig. 1). Nine GM ROIs were selected through a literature review of relevant CHR and FEP studies: anterior cingulate cortex (ACC), hippocampus, inferior frontal gyrus (IFG), medial prefrontal cortex (MPFC), middle frontal gyrus (MFG), parahippocampal gyrus, precuneus, superior frontal gyrus (SFG), and superior temporal gyrus (STG).

Texture analysis

TA was performed upon bilateral ROI masks using the 3D gray-level co-occurrence matrix (GLCM) [37]. GLCM is an N-squared matrix, in which N stands for the number of different gray level intensities within a region. GLCM is used to measure the quantitative relationship between voxels by counting the occurrences of reference voxel intensity i appearing with neighboring voxel intensity j within a predesignated distance d and direction θ. We chose the GLCM to measure texture for the following reasons: (1) GLCM texture is widely used in clinical studies, such as those with Alzheimer's Dementia (AD) and (2) the GLCM relies on relative voxel contrasts rather than other measures, such as first-order statistical texture, which relies on absolute values of signal intensity. Such characteristics of the GLCM make it less prone to interscan variability [15], which, if present, could hinder the generalization of GLCM texture. GLCM texture calculations [15] were performed using MATLAB ver. R2019b (The MathWorks, Inc., Natick, Massachusetts, USA).

First, extracted ROI images with original signal intensity values were normalized by applying the 3σ normalization method, which is widely applied in TA with the objective of removing outliers (e.g., cerebrospinal fluid, white matter) that could confound results and cause partial volume effects [15, 38]. Then, the normalized ROI images were downscaled into 32 levels of grayscale. This discretization step is routinely performed in TA, mainly to prevent a large number of zero-valued entries [23, 39]. Then, a 3D GLCM map was calculated for adjacent voxel pairs with a distance of 1 within 13 possible directions [40]. Using these 13 3D GLCM maps, each of the 22 texture features was calculated and averaged (for 13 directions), yielding 22 texture features per ROI.

Feature selection and dimensionality reduction using principal component analysis

The intercorrelation [15] among the texture features can lead to a high dimensionality problem. To address this, we initially scrutinized the

Table 1. Descriptive formulae of texture features used in this study.

Texture feature	Formula [73]	Description [73]
Inverse difference (ID)	$ID = \sum_{k=0}^{N_g-1} \frac{p_{x-y}(k)}{1+k}$	ID is a measurement of an image's local homogeneity. More uniform gray levels in an image will result in a greater overall value.
Autocorrelation (AC)	$AC = \sum_{i=1}^{N_g} \sum_{j=1}^{N_g} p(i,j)ij$	Autocorrelation measures the degree of fineness or coarseness. Higher values are produced by textures with more pairs of high gray levels.
Informational measure of correlation 1 (IMC1)	$IMC1 = \frac{HXY-HXY1}{\max\{HX,HY\}}$	IMC1 evaluates the correlation between the probability distributions of i and j (quantifying the texture's complexity) by using mutual information. Correlation is a numeric value ranging from 0 (no correlation) to 1 (perfect correlation) that indicates the linear dependence of gray level values on their respective voxels in the GLCM. Generally, higher correlation values lead to lower IMC1 values.

N_g: the number of discrete gray level intensities

p(i, j): the normalized co-occurrence matrix, which is equal to $\frac{P(i,j)}{\sum P(i,j)}$

P(i, j): the co-occurrence matrix for an arbitrary distance and angle

$p_{x-y}(k) = \sum_{i=1}^{N_g} \sum_{j=1}^{N_g} p(i,j)$, where $|i\text{-}j| = k$ and $k = 0,1, \ldots, N_g\text{-}1$

$HX = -\sum_{i=1}^{N_g} p_x(i) \log_2(p_x(i) + \epsilon)$, which is the entropy of p_x

$HY = -\sum_{i=1}^{N_g} p_y(i) \log_2(p_y(i) + \epsilon)$, which is the entropy of p_y

$HXY = -\sum_{i=1}^{N_g} \sum_{j=1}^{N_g} p(i,j) \log_2(p(i,j) + \epsilon)$, which is the entropy of $p(i,j)$

$HXY1 = -\sum_{i=1}^{N_g} \sum_{j=1}^{N_g} p(i,j) \log_2(p_x(i)p_y(j) + \epsilon)$

The Supplementary Materials of this reference article [73] contain a comprehensive description of each formula.

correlation patterns of the 22 texture features. We identified three clusters through a three-step process: a meticulous visual inspection of correlation heatmaps, unsupervised agglomerative hierarchical clustering (Supplementary Fig. 2), and evaluation of the results gleaned from the rotated component matrices derived from principal component analysis (PCA).

The most relevant texture features identified from each of the three clusters were informational measure of correlation 1 (IMC1), autocorrelation (AC), and inverse difference (ID) (Supplementary Fig. 3). These three features showed a very strong correlation with the three extracted principal components (PCs) (correlation coefficients ranging between 0.907 and 0.993). Hence, instead of the PCs, we chose to retain these original three features (IMC1, AC, and ID), thereby preserving the interpretability of the original texture features.

In-depth descriptions of the methods, procedures, and supporting materials are provided in the Supplementary Information.

Texture features

The specific calculation formulae for the three texture features employed in this study are detailed in Table 1.

IMC1 measures the correlation/complexity of voxels using mutual information. Complete independence (no correlation) between voxels equates to a value of −1, while complete dependence between voxels equates to a value of 0. AC measures the fineness/coarseness of texture, influenced by the relative intensities of voxels and their respective positions. Generally, more pairs of higher/brighter gray levels equate to larger values [31]. ID measures the degree of local homogeneity; greater uniformity results in higher values. How different patterns of gray level voxels may translate into different values of texture are illustrated in Supplementary Fig. 4.

Statistical analyses

IBM SPSS Statistics 25 (IBM, Armonk, NY, USA) was used for statistical analyses. Group differences in demographic variables were analyzed using analysis of variance and pairwise post hoc t-tests and chi-square tests. Normality assumptions of volumetric/texture measures were assessed using the Shapiro–Wilk test. For the measures that met normality assumptions, general linear model was used to assess main group effects. For the measures not meeting normality assumptions, generalized linear model was applied. For GMV and SA, the main effect of group was tested after adjusting for the effects of age, sex, and ICV. For CTh, the main effect of each group was tested after adjusting for age and sex. When testing for these main group effects, the false discovery rate (FDR) was used to correct for multiple comparison effects. Exploratory Pearson analyses with FDR corrections were used to evaluate the general relationship between the different texture-, volume-, and-surface-based measures. To test the main group effect of texture measures, age, sex, regional GMV, and CTh were entered as covariates, and FDR correction was used. For the post hoc analysis, a pairwise *t*-test with Bonferroni correction was used. To delineate the relationships between texture and symptoms, frontal texture with significant post hoc group effects were tested to determine whether they had significant correlations with positive or negative symptom subscores in the CHR (SOPS) and FEP (PANSS) groups, respectively. For this purpose, Pearson correlation with Bonferroni corrections were used.

RESULTS

Clinical and demographic characteristics of the study participants

The three study groups differed in age [$F(2,330) = 10.088$, $P < 0.001$], and the average age of participants in the CHR group was approximately 3 years younger than that of participants in the other groups (Table 2). Sex distributions were also different, with a slight male predominance observed in the CHR and HC groups.

In the FEP group, the mean duration of illness was 6.94 months (SD = 5.54), and the total PANSS score was 67.87 (SD = 16.33). Participants in the FEP group were receiving a mean olanzapine equivalent dose of 9.72 mg (SD = 7.71) [41]. CHR participants exhibited a mean total SOPS score of 34.66 (SD = 12.36).

Group differences in regional GMV, CTh, and SA

Significant main group effects of GMV and CTh were found in various frontotemporal regions (Table 3).

Post hoc analyses showed that a decrease in GMV was evident in the MPFC, SFG, MFG, IFG, hippocampus, and STG of FEP patients compared to HCs. In the CHR group, there were no significant post hoc results in regional GMVs except for the IFG. Post hoc results showed that CTh was decreased in the MPFC, SFG, MFG, IFG, and the STG in the FEP group in relation to both the CHR and HC groups.

Relationship between texture, cortical thickness, regional volume, and age

While GLCM texture features are thought to be correlated with volume measures [22], their exact relationships have not been properly investigated. Exploratory Pearson correlation analyses were performed to examine the relationships between different volumetric measures, texture, and age (Supplementary Table 3).

Weak associations between IMC1 and volume, between AC and thickness, and between ID and thickness were found in the MPFC, SFG, and MFG. None of the texture features showed significant associations with age; however, frontal GMV and CTh were moderately associated with age (Supplementary Table 4).

Table 2. Clinical and demographic variables of the study participants.

	FEP ($n = 101$)	CHR ($n = 85$)	HC ($n = 147$)	Statistics	
				F or χ^2	*P* value
Age (years)	23.54 ± 5.82	20.66 ± 3.84	23.39 ± 4.89	10.088	<0.001
Sex (male/female)	50/51	63/22	97/50	12.969	0.002
DOI (months)	6.98 ± 5.54				
Total PANSS score	67.87 ± 16.33				
Positive symptoms	16.38± 5.31				
Negative symptoms	17.58 ± 6.01				
General symptoms	33.90 ± 8.35				
Total SOPS score		34.66 ± 12.36			
Positive symptoms		9.89 ± 3.69			
Negative symptoms		13.61 ± 6.33			
Disorganization		4.19 ± 2.79			
General symptoms		6.98 ± 4.33			
Antipsychotic dose (mg)[a]	9.72 ± 7.71	0			
Intracranial volume (cm^3)	1580 ± 147	1631 ± 147	1600 ± 157	2.632	0.073

HC healthy control, *CHR* clinical high risk for psychosis, *FEP* first-episode psychosis, *DOI* duration of untreated illness, *PANSS* Positive and Negative Symptom Scale, *SOPS* Scale of Prodromal Symptom.
[a]Antipsychotic dose is stated as the olanzapine equivalent dose [41].

Separate correlation analyses were also performed in each of the study groups (Supplementary Tables 5–7). Similar patterns of association between IMC1 and volume, between AC and thickness, and between ID and thickness in the MPFC, SFG, and MFG were found in FEP patients and HCs. In the CHR group, however, texture was not associated with either volume or thickness.

Group differences in texture features

The main group effects were tested using texture features of the six ROIs that showed significant group differences in GMV and CTh (Table 4). Significant group effects were found in the IMC1 textures of all 6 ROIs. The effects of AC and ID were restricted to the frontal subregions.

Post hoc analysis revealed a significant and consistent increase in frontal IMC1 (i.e., less correlation and more complexity) in the CHR compared to the HC group. Additionally, AC increases (i.e., increased coarseness) in the MPFC, SFG, and MFG were found in the FEP compared with the HC group, and the ID was decreased in the MPFC (i.e., decreased homogeneity) in CHR individuals compared with HCs.

Association of psychotic symptoms and texture features

In the FEP group, there were no significant correlations between symptom subscores and texture features.

In the CHR group, a smaller SOPS positive subscore was associated with larger values of IMC1 textures in the MFG ($r = -0.447$, $P < 0.001$, P-Bonferroni < 0.001), MPFC ($r = -0.370$, $P < 0.001$, P-Bonferroni = 0.016), and SFG ($r = -0.363$, $P < 0.001$, P-Bonferroni = 0.021); however, this association was not observed in the regional GMVs or CTh measures (Fig. 1).

DISCUSSION

In this study, we performed TA on psychosis-affected GM regions to investigate the utility of texture in the early stages of psychosis. First, we found that frontotemporal GM abnormalities were evident only in FEP (and not in the CHR group) compared with HCs. Namely, a significant decrease in CTh in the FEP compared to both the CHR and HC groups and a decrease in GMV in the FEP compared to the HC group were observed. These results are in line with previous reports in the literature, in which a pronounced decrease in frontotemporal GMV/CTh *after* psychosis onset with mixed findings of a decrease in GMV/CTh in the CHR period has been observed [7–11, 42]. Second, an increase in frontal AC texture was found in FEP patients compared to HCs after adjusting for changes in GMV/CTh. Third, we identified a distinctive and consistent pattern of increased frontal IMC1 texture in the CHR group that remained significant even after controlling for the effects of GMV/CTh measures. The pattern of increase in frontal IMC1 texture in the CHR group was stagewise nonlinear; it exceeded both the controls and FEP group. Increased frontal IMC1 was also associated with a lesser severity of attenuated positive symptoms in the CHR group; however, neither GMV nor CTh shared this association.

Interpretation of GMV and CTh findings

Accumulated evidence points to frontotemporal GM abnormalities as an established finding in patients with FEP [4] and chronic schizophrenia [43]. In CHR studies, however, such GM abnormalities are more varied, with reports of decreased [7–10], equivocal [11], or even increased [10, 42] GMV findings. The results of our study support the extant literature, given that a frontotemporal GMV decrease was evident only in the FEP group (and not in the CHR group) compared with the controls. Such discrepancies in the GM findings between CHR and FEP patients may result from the presence of subtle GM changes in the CHR period not overt enough to be reflected as GMV/CTh changes. The results of a recent mega-analysis by the ENIGMA working group also support this notion, showing that while the CHR group exhibited a widespread decrease in CTh, the degree of decrease was subtle [30].

Meanwhile, previous studies have provided evidence of T1 GM intensity alterations in patients with schizophrenia [44, 45], in which the degree of alterations was observed to be either similar to [46] or in excess of the degree of cortical thinning [47]. Moreover, a recent publication found that T1 GM intensity was altered in the absence of significant CTh changes in CHR [11], suggesting these measures could be more sensitive than GMV/CTh in these early stages. Since GLCM texture is calculated with

Table 3. Regional gray matter volume, cortical thickness, and surface area values of study participants.

	HC ($n = 147$)[a]	CHR ($n = 85$)[b]	FEP ($n = 101$)[c]	F[d] or Wald $\chi 2$[e]	*p* value	*p*-FDR[f]	Post hoc[g]
Gray matter volume							
Anterior cingulate cortex	9889 ± 105	9905 ± 150	9803 ± 119	0.198	0.820	0.985	–
Medial prefrontal cortex	62530 ± 373	61890 ± 532	60689 ± 422	5.481	0.005	0.019*	c < a
Superior frontal gyrus	52640 ± 338	51985 ± 482	50886 ± 383	6.039	0.003	0.028*	c < a
Middle frontal gyrus	51716 ± 344	51205 ± 492	50126 ± 390	4.811	0.009	0.029*	c < a
Inferior frontal gyrus	25709 ± 215	25796 ± 308	24726 ± 244	5.704	0.004	0.019*	c < a, b
Hippocampus	9608 ± 54	9472 ± 77	9272 ± 61	8.493	<0.001	0.003**	c < a
Parahippocampal gyrus	4349 ± 43	4368 ± 62	4342 ± 49	0.055	0.946	0.985	–
Superior temporal gyrus	28926 ± 218	28612 ± 312	27695 ± 247	7.280	0.001	0.008**	c < a
Precuneus	22813 ± 161	23132 ± 217	22937 ± 189	1.459	0.482	0.770	–
Cortical thickness							
Anterior cingulate cortex	2.720 ± 0.011	2.713 ± 0.016	2.681 ± 0.012	3.362	0.050	0.126	–
Medial prefrontal cortex	2.913 ± 0.010	2.912 ± 0.014	2.842 ± 0.011	14.750	<0.001	<0.001***	c < a, b
Superior frontal gyrus	2.952 ± 0.010	2.953 ± 0.015	2.875 ± 0.012	14.950	<0.001	<0.001***	c < a, b
Middle frontal gyrus	2.559 ± 0.008	2.543 ± 0.012	2.488 ± 0.010	21.466	<0.001	<0.001***	c < a, b
Inferior frontal gyrus	2.689 ± 0.009	2.683 ± 0.013	2.626 ± 0.010	19.857	<0.001	<0.001***	c < a, b
Parahippocampal gyrus	2.590 ± 0.019	2.575 ± 0.027	2.585 ± 0.021	0.475	0.904	0.985	–
Superior temporal gyrus	2.896 ± 0.010	2.911 ± 0.014	2.819 ± 0.013	26.889	<0.001	<0.001***	c < a, b
Precuneus	2.439 ± 0.009	2.424 ± 0.013	2.408 ± 0.010	9.842	0.067	0.146	–
Surface area							
Anterior cingulate cortex	2942 + 30	2967 ± 43	2975 ± 34	0.286	0.752	0.940	–
Medial prefrontal cortex	17534 ± 109	17501 ± 156	17522 ± 123	0.015	0.985	0.985	–
Superior frontal gyrus	14568 ± 128	14824 ± 168	14383 ± 154	3.732	0.155	0.242	–
Middle frontal gyrus	14838 ± 103	14891 ± 147	14909 ± 117	0.114	0.892	0.985	–
Inferior frontal gyrus	7720 ± 72	8017 ± 95	7572 ± 87	12.203	0.002	0.007***	b > a, c
Parahippocampal gyrus	1338 ± 13	1369 ± 17	1328 ± 15	3.296	0.192	0.282	–
Superior temporal gyrus	8122 ± 49	8140 ± 71	8050 ± 56	0.654	0.521	0.724	–
Precuneus	8179 ± 72	8439 ± 104	8414 ± 82	3.208	0.042	0.081	–

HC healthy control, *CHR* clinical high risk, *FEP* first-episode psychosis, *FDR* false discovery rate.
*p-FDR < 0.05, **p-FDR < 0.01, ***p-FDR < 0.001.
[a,b,c]refer to those respective groups in the post hoc analysis results.
[d]General linear model or [e]generalized linear model to test for the main effect of group. For the regional volumes and surface area, age, sex, and intracranial volumes were entered as covariates. For cortical thickness, age and sex were entered as covariates.
[f]Multiple correction was performed using the false discovery rate (FDR).
[g]Pairwise comparison with Bonferroni correction.

regard to various properties of underlying T1 GM intensities, it may detect subtle and miniscule changes with greater sensitivity than a single metric (GMV, CTh, GM intensity) [15, 22].

Interpretation of how texture may reflect the underlying cortical structure of the first-episode psychosis group

It is important to note that caution should be taken when interpreting the meaning of texture in the absence of histological data. However, T1 signal intensity is known to be sensitive to changes in the underlying tissue microstructure, such as the content of myelin, cell density, size of neurons, and free water [48]. Of them, T1 signal intensity is known to be particularly dependent on changes in the brain myeloarchitecture [48]. Possible explanations for increased frontal AC in the FEP group include changes in (1) the macrostructural cortical lamina, (2) the amount/density of neuropil, and (3) cortical myelination. Figure 2 demonstrates a proposed schematic explanation of texture and volume changes occurring in the early-stage psychosis.

First, changes in the macrostructural cortical lamina may have contributed to the texture change in the FEP group. Since human GM CTh varies between 1.6–4.5 mm with the frontal cortex being the thickest [49], the normal laminar structure of the frontal cortex is assumed to be three-to-five voxel-layers deep. Deeper layers of GM cortex are more densely myelinated [50], resulting in higher/brighter T1 intensity. Because GMV decreases in schizophrenia are thought to be mainly driven by cortical thinning occurring most prominently in layers II and III [51–53], the frontal cortical structure of the FEP group with decreased GMV may be conceptualized as being approximately two-to-three voxel-layers deep [54]. These decreases in GMV/CTh may accompany changes in AC texture. In other words, an increase in AC may result from the disproportionate thinning of different cortical layers (leading to overall changes in the relationship between different cortical and voxel layers). More specifically, as presented in Fig. 2, the GMV decrease in FEP patients may have caused alterations in the upper cortical layers (II and III), resulting in a higher signal intensity than that observed in controls. This explanation is also supported by the results of our exploratory correlation analysis (Supplementary Table 3), which demonstrated a consistent negative association between frontal AC and CTh.

Another factor that might contribute to texture changes in the FEP group includes changes in microstructural organization. In

Table 4. Main group effects and post hoc results for regional texture features.

Region and texture features	HC ($n = 147$)[a]	CHR ($n = 85$)[b]	FEP ($n = 101$)[c]	Statistics[d, e]			
				F[d] or Wald $\chi 2$[e]	p value[f]	p-FDR	Post hoc[g]
IMC 1							
Frontal							
MPFC	−0.181 ± 0.003	−0.156 ± 0.005	−0.172 ± 0.004	8.711	<0.001	0.003**	b > a
SFG	−0.148 ± 0.003	−0.129 ± 0.004	−0.140 ± 0.004	7.346	0.001	0.009**	b > a
MFG	−0.114 ± 0.002	−0.101 ± 0.003	−0.112 ± 0.003	6.171	0.002	0.009**	b > a, c
IFG	−0.125 ± 0.002	−0.110 ± 0.003	−0.115 ± 0.003	11.533	0.003	0.009**	b > a, c
Temporal							
STG	−0.069 ± 0.002	−0.081 ± 0.003	−0.072 ± 0.002	10.811	0.004	0.010*	b < a
Hippocampus[h]	−0.042 ± 0.001	−0.046 ± 0.001	−0.046 ± 0.001	12.510	0.002	0.009**	b, c < a
Autocorrelation							
Frontal							
MPFC	305.21 ± 14.57	356.91 ± 19.62	364.26 ± 17.76	8.431	0.015	0.030*	c > a
SFG	237.92 ± 14.07	292.63 ± 19.01	300.30 ± 17.16	10.095	0.006	0.013*	c > a
MFG	266.84 ± 16.11	346.39 ± 21.50	332.20 ± 19.66	11.593	0.003	0.009**	b, c > a
IFG	512.57 ± 17.53	574.93 ± 23.55	560.57 ± 21.28	5.812	0.055	0.083	–
Temporal							
STG	610.67 ± 22.50	579.01 ± 30.22	571.06 ± 27.09	1.504	0.471	0.499	–
Hippocampus[h]	371.89 ± 15.56	399.33 ± 21.02	351.48 ± 18.77	2.805	0.240	0.270	–
ID							
Frontal							
MPFC	0.793 ± 0.004	0.776 ± 0.005	0.780 ± 0.005	7.211	0.027	0.044*	b < a
SFG	0.793 ± 0.005	0.771 ± 0.007	0.772 ± 0.006	8.141	0.017	0.031*	–
MFG	0.769 ± 0.005	0.753 ± 0.007	0.756 ± 0.006	3.397	0.183	0.220	–
IFG	0.769 ± 0.004	0.779 ± 0.005	0.782 ± 0.004	4.459	0.108	0.143	–
Temporal							
STG	0.846 ± 0.005	0.859 ± 0.007	0.865 ± 0.007	4.395	0.111	0.143	–
Hippocampus[h]	0.907 ± 0.004	0.908 ± 0.006	0.901 ± 0.005	1.103	0.577	0.577	–

*p-FDR < 0.05, **p-FDR < 0.01.
[a,b,c]refer to those respective groups in the post hoc analysis results. Groupwise texture values are presented as the estimated average ± standard error after controlling for the effects of the confounding variables.
[d]General linear model or [e]generalized linear model to test for the main effect of group after adjusting for the effects of age, sex, regional volume and cortical thickness.
[f]Results of multiple regression were corrected with the false discovery rate. Those with a corrected p level ≤ 0.05 were considered significant.
[g]Pairwise comparison with Bonferroni correction.
[h]For the hippocampus, the effects of age, sex, and regional volume were adjusted.

postmortem studies of patients with chronic schizophrenia, cortical layer III abnormalities (decreases in neuronal size, dendrite density, and neuropil) are most consistently reported [55, 56]. Findings of abnormal oligodendrocytes in cortical layers III, V, and VI [57, 58] are also widely replicated in patients with schizophrenia. It is important to note that the results of these postmortem studies, which primarily include chronic patients, are not directly transferrable to the interpretation of texture changes observed in FEP patients. However, accumulating evidence from in vivo neuroimaging studies also supports the presence of GM microstructure disruption in both patients with FEP and schizophrenia [59, 60], implicating disrupted cortical myelination and altered cytoarchitecture mainly in the frontotemporal areas [59, 60]. From these results, the following inferences can be made: changes in both macroscopic and microstructural organizations of GM can be measured by MRI, even as early in the FEP period.

Abnormalities in AC have been implicated in other central nervous disorders [31, 61–63], and one study has suggested a possible link to abnormal intracortical myelination [31]. While current evidence on the findings of intracortical myelin in patients with schizophrenia is inconclusive, the most recent publication utilizing myelin-specific imaging demonstrated increased markers of intracortical myelin in the midcortical layers within the prefrontal regions [64]. Moreover, while intracortical myelination increases from adolescence to middle-late adulthood during normal development [65], aberrant increases are thought to hinder new dendrite formation, thereby leading to decreased plasticity and disruption of local circuitry [66]; this corresponds with the modern understanding of schizophrenia as a disconnection syndrome. Increased frontal AC in the FEP group may either reflect changes in cytoarchitecture or intracortical myelination or possibly changes in both (i.e., intermittent occurrence of lighter gray voxels between generally darker backgrounds of GM). It is also pertinent to note that, in terms of T1 contrast, both the decrease in neuropil (including somal size and dendrites) and the increase in cortical myelination can result in higher T1 signal intensity [67].

Hypothesized implications of texture in the CHR group

Because the actual histology and cytoarchitecture of the at-risk states cannot be ascertained due to the lack of postmortem

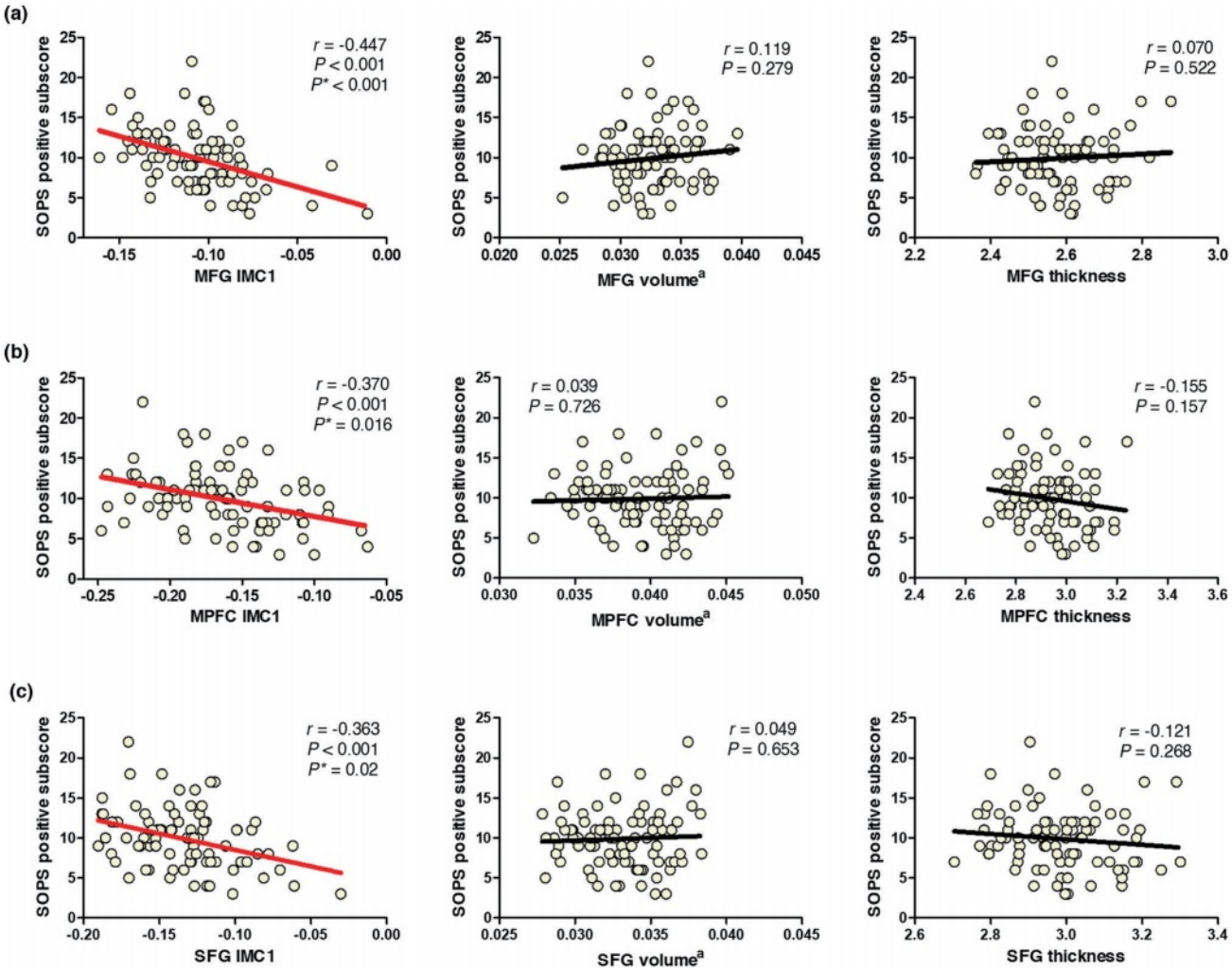

Fig. 1 Association of attenuated positive symptom severity in the clinical high-risk group with texture/volumetric features. Texture was negatively associated with positive SOPS subscores, while regional volumes and cortical thickness were not. **a** Middle frontal gyrus. **b** Medial prefrontal cortex. **c** Superior frontal gyrus. a Gray matter volume adjusted for by the intracranial volumes. P* *P* value after Bonferroni correction. SOPS Scale of Prodromal Symptoms, IMC1 informational measure of correlation 1.

studies, interpretation of the effects of a dyscorrelated pattern of frontal texture in patients at CHR is difficult. We suggest two possible explanations. First, increased IMC1 in the CHR group could reflect cytoarchitectural abnormalities present at above a subthreshold level (e.g., aberrant intracortical myelin, decreased somal size, dendrite density, and neuropil). The second possibility is that the results of a stagewise nonlinear increase in frontal IMC1 may reflect a dynamic reorganization process. Namely, we suggest that the less correlated, less interdependent voxel relationships as reflected by the increased IMC1 in the CHR group may be a reflection of a more dynamic, predisorder cortex as opposed to the more static/stabilized cortex seen in both HCs and FEP groups (i.e., more correlated and interdependent local voxel relationships are reflected by a smaller IMC1).

Human cortex undergoes a constant reorganization process during exposure to both normative and pathological stimuli [67]. In terms of disease process, such a reorganization process could reflect either consolidation or resilience to disease states depending on the functional outcome [68, 69]. Since CHR represents a subthreshold prodromal period that could result in remission or a transition into psychosis, the pattern of dyscorrelated cortical texture (i.e., an increase in the appearance of voxels that are independent of nearby voxels) in this group may reflect that a dynamic reorganization process is in place (e.g., formation or elimination of synapses/dendrites, shrinkage of large neurons, myelination, demyelination, or even reactive myelination) [70], occurring before pathological changes become more prominent and consolidated (e.g., overt decreases in GMV/CTh).

Some seemingly contradicting previous reports of increased GMV in CHR and FEP patients have also implied that such a reorganization process may take place. Dukart and colleagues reported distributed regional GMV increases (mainly in the frontotemporal regions) in CHR and FEP groups compared to controls [42]. A commentary regarding these findings by Palaniyappan and colleagues highlighted the possible role of the ameliorative reorganization process, which "may underlie the physiology of compensation and resilience" [71]. If such compensatory reorganization processes are indeed present in the CHR stage, our results may provide useful insights into understanding the structural determinants of either progression or resilience to psychotic illness.

Different patterns of texture alterations in the temporal regions

The variation in cortical architecture may have led to a different pattern of alterations in the temporal texture compared to the frontal areas. These differences are discussed in further detail in the Supplementary Information.

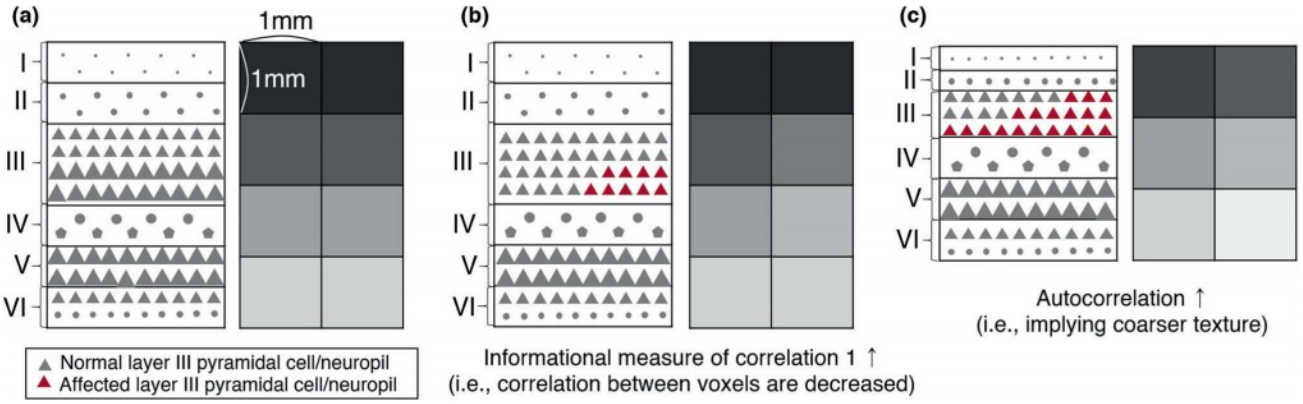

Fig. 2 Schematic illustration of the study findings. a Normal cytoarchitecture (left) and texture (right) of the frontal cortex. Voxel contrast, which is determined by T1 signal intensity, is sensitive to tissue myelin content. Thus, the texture matrices of cortical layers IV, V, and VI, which contain abundant intracortical myelin, result in higher (i.e., brighter) gray levels. This spectral ordering from darker to brighter voxel intensities [50] forms a uniform, fine cortical texture. **b** Proposed cytoarchitecture and texture of clinical high-risk individuals. Total volume and cortical thickness are relatively preserved (i.e., unchanged or subthreshold decreases). Either of the following two cytoarchitectural factors may contribute to the more dyscorrelated cortical texture found in this group. First, subtle changes in underlying cells and tissues (e.g., subthreshold decreases in dendrite density, neuropil, somal size) may be present (depicted as dark red triangles). Second, it may be a result of compensatory, reorganization processes (e.g., formation/elimination of synapses/dendrites, shrinkage of large neurons, myelination, demyelination, or even reactive myelination). **c** Proposed cytoarchitecture and texture of patients with first-episode psychosis. First, total volume and cortical thickness are decreased; this decrease is mostly driven by changes occurring in cortical layers II and III. This results in a decrease in the number of voxels in the texture matrix (i.e., four voxels deep → three voxels deep). This also results in an overall spatial pattern change in which rows of voxels represent layers of the cortex. Second, somal size, dendrite density, and the corresponding neuropil are decreased (up to 23%) [74] in deep layer III (depicted as dark red triangles). Third, oligodendrial abnormalities found in layers III, V, and VI may result in aberrant intracortical myelination. Such overall cytoarchitectural changes may be reflected upon texture changes, resulting in a coarser cortical texture.

Strengths and limitations

To our knowledge, this is the first study to investigate the relationship between GM texture and disease stage, volumetric measures (GMV, CTh, SA), age, and clinical symptoms in CHR and FEP patients. Crucially, previous studies have predominantly examined whole-brain images, presenting a challenge in attributing whole-brain texture changes to GM abnormalities due to the spatial and volumetric compression of GM compared to white matter and ventricular spaces. Our study is the first to systematically explore GM texture abnormalities in early-stage psychosis, augmenting the novelty of our findings and methods. Furthermore, our results indicate a relatively strong and consistent association between increased frontal IMC1 and reduced severity of attenuated positive symptoms, suggesting that texture may be an indicator of CHR symptomatology that has greater sensitivity than volume/CTh. This is the first study in psychosis or schizophrenia research to link the symptoms in the CHR stage consistently with GM texture. Our results also suggest the possibility of a dynamic reorganization process during the CHR period, which has the potential to make significant contributions to the field by illuminating new aspects of GM changes during the early-stage psychosis. However, this study had several limitations with some implications for future studies.

First, the meaning of texture could not be directly inferred since histological data were not available. While this precludes delineating the specific origin of texture changes, results do suggest that texture provides more information than volumetric measures alone. Since GM decreases in psychosis are assumed to be a complex process that is not driven by a single factor [51, 56, 67, 71], texture may provide a unique snapshot of GM changes that occur both macro- and micro-structurally. Magnetic resonance texture studies utilizing specific animal models of psychosis may provide a greater understanding of the specific histological background of texture.

Second, MRI data used in this study were collected cross-sectionally in a single center, which limits the generalizability of the results. Nevertheless, GLCM texture is thought to be less influenced by interscanner effects and more generalizable than other radiomic/texture features, such as first-order statistics [15]. Additionally, while not directly comparable, a previous oncologic radiomic/texture study utilizing large-scale multicenter imaging data demonstrated these features not only were stable and reproducible but also held translational capabilities across different tumor types [72].

Third, it cannot be inferred from the findings of this study alone if the results represent a psychosis-specific abnormality. While the CHR group in this study were not receiving any antipsychotic medications, most patients with FEP were receiving them. However, AC texture has also been implicated in other central nervous system disorders in at least four previous studies [21, 31, 61–63]. If the widely different etiology/pathophysiology of these disorders – AD, amyotrophic lateral sclerosis, dementia with Lewy bodies, psychosis – are considered, texture abnormalities common to these different disorders (AC) are more likely to imply a relationship with downstream neural changes (e.g., myelination or change in the amount of neuropil) rather than the effects of medication or disease specificity. On the other hand, IMC1 might be a measure with greater sensitivity that is capable of detecting subtle and possibly dynamic changes in the GM even in the absence of overt changes in GMV/CTh. Future studies should investigate whether these texture changes occur in a psychosis-specific manner.

In conclusion, this study investigated the utility of texture and its relationship with volume, CTh, age, and clinical symptoms in subjects with early-stage psychosis. The results of volumetric and CTh analyses indicated overt frontotemporal GM abnormalities in the FEP but not in the CHR group; these findings support the extant literature. The TA results revealed a consistent and distinctive pattern of increased frontal IMC1 in the CHR group that remained significant even after controlling for the effects of volume and CTh. Furthermore, we found a relatively strong and consistent associations between increased frontal IMC1 and reduced severity of attenuated positive symptoms in the CHR group. Possible implications of these texture alterations are

discussed in terms of structural organization of the GM and their hypothesized functions. These findings suggest that frontal IMC1 texture may be an indicator of both symptomatology and dynamic GM changes occurring during the CHR period that has greater sensitivity than volume/CTh. This study highlights the potential of texture as a useful tool to investigate subtle GM changes in early-stage psychosis.

REFERENCES

1. Andreasen NC, Nopoulos P, Magnotta V, Pierson R, Ziebell S, Ho B-C. Progressive brain change in schizophrenia: a prospective longitudinal study of first-episode schizophrenia. Biol Psychiatry. 2011;70:672–9.
2. Vita A, De Peri L, Deste G, Sacchetti E. Progressive loss of cortical gray matter in schizophrenia: a meta-analysis and meta-regression of longitudinal MRI studies. Transl Psychiatry. 2012;2:e190.
3. Van Haren NE, Schnack HG, Cahn W, Van Den Heuvel MP, Lepage C, Collins L, et al. Changes in cortical thickness during the course of illness in schizophrenia. Arch Gen Psychiatry. 2011;68:871–80.
4. Zipursky RB, Lambe EK, Kapur S, Mikulis DJ. Cerebral gray matter volume deficits in first episode psychosis. Arch Gen Psychiatry. 1998;55:540–6.
5. Job DE, Whalley HC, McConnell S, Glabus M, Johnstone EC, Lawrie SM. Structural gray matter differences between first-episode schizophrenics and normal controls using voxel-based morphometry. Neuroimage. 2002;17:880–9.
6. Hulshoff Pol HE, Kahn RS. What happens after the first episode? A review of progressive brain changes in chronically ill patients with schizophrenia. Schizophr Bull. 2008;34:354–66.
7. Fusar-Poli P, Borgwardt S, Crescini A, Deste G, Kempton MJ, Lawrie S, et al. Neuroanatomy of vulnerability to psychosis: a voxel-based meta-analysis. Neurosci Biobehav Rev. 2011;35:1175–85.
8. Mechelli A, Riecher-Rössler A, Meisenzahl EM, Tognin S, Wood SJ, Borgwardt SJ, et al. Neuroanatomical abnormalities that predate the onset of psychosis: a multicenter study. Arch Gen Psychiatry. 2011;68:489–95.
9. Iwashiro N, Suga M, Takano Y, Inoue H, Natsubori T, Satomura Y, et al. Localized gray matter volume reductions in the pars triangularis of the inferior frontal gyrus in individuals at clinical high-risk for psychosis and first episode for schizophrenia. Schizophr Res. 2012;137:124–31.
10. Ding Y, Ou Y, Pan P, Shan X, Chen J, Liu F, et al. Brain structural abnormalities as potential markers for detecting individuals with ultra-high risk for psychosis: a systematic review and meta-analysis. Schizophr Res. 2019;209:22–31.
11. Zikidi K, Gajwani R, Gross J, Gumley AI, Lawrie SM, Schwannauer M, et al. Grey-matter abnormalities in clinical high-risk participants for psychosis. Schizophr Res. 2020;226:120–8.
12. Cropley VL, Lin A, Nelson B, Reniers RL, Yung AR, Bartholomeusz CF, et al. Baseline grey matter volume of non-transitioned "ultra high risk" for psychosis individuals with and without attenuated psychotic symptoms at long-term follow-up. Schizophr Res. 2016;173:152–8.
13. Chung Y, Jacobson A, He G, van Erp TG, McEwen S, Addington J, et al. Prodromal symptom severity predicts accelerated gray matter reduction and third ventricle expansion among clinically high-risk youth developing psychotic disorders. Complex Psychiatry. 2015;1:13–22.
14. Walter A, Studerus E, Smieskova R, Kuster P, Aston J, Lang UE, et al. Hippocampal volume in subjects at high risk of psychosis: a longitudinal MRI study. Schizophr Res. 2012;142:217–22.
15. Lee S, Lee H, Kim KW. Magnetic resonance imaging texture predicts progression to dementia due to Alzheimer disease earlier than hippocampal volume. J Psychiatry Neurosci. 2020;45:7–14.
16. Depeursinge A, Foncubierta-Rodriguez A, Van De Ville D, Müller H. Three-dimensional solid texture analysis in biomedical imaging: review and opportunities. Med Image Anal. 2014;18:176–96.
17. Aerts HJ. The potential of radiomic-based phenotyping in precision medicine: a review. JAMA Oncol. 2016;2:1636–42.
18. Fan Y, Feng M, Wang R. Application of radiomics in central nervous system diseases: a systematic literature review. Clin Neurol Neurosurg. 2019;187:105565.
19. Zhang Y, Zhu H, Mitchell JR, Costello F, Metz LM. T2 MRI texture analysis is a sensitive measure of tissue injury and recovery resulting from acute inflammatory lesions in multiple sclerosis. Neuroimage. 2009;47:107–11.
20. Holli KK, Wäljas M, Harrison L, Liimatainen S, Luukkaala T, Ryymin P, et al. Mild traumatic brain injury: tissue texture analysis correlated to neuropsychological and DTI findings. Acad Radiol. 2010;17:1096–102.
21. Ishaque A, Mah D, Seres P, Luk C, Johnston W, Chenji S, et al. Corticospinal tract degeneration in ALS unmasked in T1-weighted images using texture analysis. Hum Brain Mapp. 2019;40:1174–83.
22. Sørensen L, Igel C, Liv Hansen N, Osler M, Lauritzen M, Rostrup E, et al. Early detection of Alzheimer's disease using M RI hippocampal texture. Hum Brain Mapp. 2016;37:1148–61.
23. Kassner A, Thornhill R. Texture analysis: a review of neurologic MR imaging applications. Am J Neuroradiol. 2010;31:809–16.
24. Ganeshan B, Miles KA, Young RC, Chatwin CR, Gurling HM, Critchley HD. Three-dimensional textural analysis of brain images reveals distributed grey-matter abnormalities in schizophrenia. Eur Radiol. 2010;20:941–8.
25. Radulescu E, Ganeshan B, Shergill SS, Medford N, Chatwin C, Young RC, et al. Grey-matter texture abnormalities and reduced hippocampal volume are distinguishing features of schizophrenia. Psychiatry Res Neuroimaging. 2014;223:179–86.
26. Latha M, Kavitha G. Segmentation and texture analysis of structural biomarkers using neighborhood-clustering-based level set in MRI of the schizophrenic brain. Magn Reson Mater Phys Biol Med. 2018;31:483–99.
27. Korda A, Ruef A, Neufang S, Davatzikos C, Borgwardt S, Meisenzahl E, et al. Identification of voxel-based texture abnormalities as new biomarkers for schizophrenia and major depressive patients using layer-wise relevance propagation on deep learning decisions. Psychiatry Res Neuroimaging. 2021;313:111303.
28. Korda AI, Andreou C, Rogg HV, Avram M, Ruef A, Davatzikos C, et al. Identification of texture MRI brain abnormalities on first-episode psychosis and clinical high-risk subjects using explainable artificial intelligence. Transl Psychiatry. 2022;12:481.
29. Park YW, Choi D, Lee J, Ahn SS, Lee S-K, Lee S-H, et al. Differentiating patients with schizophrenia from healthy controls by hippocampal subfields using radiomics. Schizophr Res. 2020;223:337–44.
30. Jalbrzikowski M, Hayes RA, Wood SJ, Nordholm D, Zhou JH, Fusar-Poli P, et al. Association of structural magnetic resonance imaging measures with psychosis onset in individuals at clinical high risk for developing psychosis: an ENIGMA working group mega-analysis: an ENIGMA working group mega-analysis. JAMA Psychiatry. 2021;78:753–66.
31. Lee S, Kim KW. Initiative ftAsDN. Associations between texture of T1-weighted magnetic resonance imaging and radiographic pathologies in Alzheimer's disease. Eur J Neurol. 2021;28:735–44.
32. Lee TY, Hwang WJ, Kim NS, Park I, Lho SK, Moon S-Y, et al. Prediction of psychosis: model development and internal validation of a personalized risk calculator. Psychol Med. 2020;52:1–9.
33. Yi J-S, Ahn Y-M, Shin H-K, An S-K, Joo Y-H, Kim S-H, et al. Reliability and validity of the Korean version of the Positive and Negative Syndrome Scale. J Korean Neuropsychiatr Assoc. 2001;40:1090–105.
34. Jung MH, Jang JH, Kang D-H, Choi J-S, Shin NY, Kim HS, et al. The reliability and validity of the Korean version of the structured interview for prodromal syndrome. Psychiatry Investig. 2010;7:257.
35. Lobbestael J, Leurgans M, Arntz A. Inter-rater reliability of the Structured Clinical Interview for DSM-IV Axis I disorders (SCID I) and Axis II disorders (SCID II). Clin Psychol Psychother. 2011;18:75–9.
36. Schwarz CG, Gunter JL, Wiste HJ, Przybelski SA, Weigand SD, Ward CP, et al. A large-scale comparison of cortical thickness and volume methods for measuring Alzheimer's disease severity. NeuroImage Clin. 2016;11:802–12.
37. Haralick RM, Shanmugam K, Dinstein IH. Textural features for image classification. IEEE Trans Syst Man Cybern. 1973;6:610–21.
38. Collewet G, Strzelecki M, Mariette F. Influence of MRI acquisition protocols and image intensity normalization methods on texture classification. Magn Reson Imaging. 2004;22:81–91.
39. Mahmoud-Ghoneim D, Alkaabi MK, de Certaines JD, Goettsche F-M. The impact of image dynamic range on texture classification of brain white matter. BMC Med Imaging. 2008;8:1–8.
40. Ortiz A, Palacio AA, Górriz JM, Ramírez J, Salas-González D. Segmentation of brain MRI using SOM-FCM-based method and 3D statistical descriptors. Comput Math Methods Med. 2013;2013.
41. Gardner DM, Murphy AL, O'Donnell H, Centorrino F, Baldessarini RJ. International consensus study of antipsychotic dosing. Am J Psychiatry. 2010;167:686–93.
42. Dukart J, Smieskova R, Harrisberger F, Lenz C, Schmidt A, Walter A, et al. Age-related brain structural alterations as an intermediate phenotype of psychosis. J Psychiatry Neurosci JPN. 2017;42:307.
43. Gupta CN, Calhoun VD, Rachakonda S, Chen J, Patel V, Liu J, et al. Patterns of gray matter abnormalities in schizophrenia based on an international mega-analysis. Schizophr Bull. 2015;41:1133–42.
44. Wolkin A, Rusinek H, Vaid G, Arena L, Lafargue T, Sanfilipo M, et al. Structural magnetic resonance image averaging in schizophrenia. Am J Psychiatry. 1998;155:1064–73.
45. Lawrie S, Abukmeil S, Chiswick A, Egan V, Santosh C, Best J. Qualitative cerebral morphology in schizophrenia: a magnetic resonance imaging study and systematic literature review. Schizophr Res. 1997;25:155–66.

46. Rosa P, Zanetti M, Duran F, Santos L, Menezes P, Scazufca M, et al. What determines continuing grey matter changes in first-episode schizophrenia and affective psychosis? Psychol Med. 2015;45:817–28.
47. van Haren NE, Cahn W, Pol HH, Kahn R. Schizophrenia as a progressive brain disease. Eur Psychiatry. 2008;23:245–54.
48. Does MD. Inferring brain tissue composition and microstructure via MR relaxometry. NeuroImage. 2018;182:136–48.
49. Fischl B, Dale AM. Measuring the thickness of the human cerebral cortex from magnetic resonance images. Proc Natl Acad Sci. 2000;97:11050–5.
50. Sprooten E, O'Halloran R, Dinse J, Lee WH, Moser DA, Doucet GE, et al. Depth-dependent intracortical myelin organization in the living human brain determined by in vivo ultra-high field magnetic resonance imaging. NeuroImage. 2019;185:27–34.
51. Harrison PJ. The neuropathology of schizophrenia: a critical review of the data and their interpretation. Brain. 1999;122:593–624.
52. Wagstyl K, Ronan L, Whitaker K, Goodyer I, Roberts N, Crow T, et al. Multiple markers of cortical morphology reveal evidence of supragranular thinning in schizophrenia. Transl Psychiatry. 2016;6:e780.
53. Williams M, Chaudhry R, Perera S, Pearce R, Hirsch S, Ansorge O, et al. Changes in cortical thickness in the frontal lobes in schizophrenia are a result of thinning of pyramidal cell layers. Eur Arch Psychiatry Clin Neurosci. 2013;263:25–39.
54. Wiegand LC, Warfield SK, Levitt JJ, Hirayasu Y, Salisbury DF, Heckers S, et al. Prefrontal cortical thickness in first-episode psychosis: a magnetic resonance imaging study. Biol Psychiatry. 2004;55:131–40.
55. Bakhshi K, Chance S. The neuropathology of schizophrenia: a selective review of past studies and emerging themes in brain structure and cytoarchitecture. Neurosci. 2015;303:82–102.
56. Harrison PJ. Postmortem studies in schizophrenia. Dialog Clin Neurosci. 2022;2:349–57.
57. Uranova NA, Vostrikov VM, Orlovskaya DD, Rachmanova VI. Oligodendroglial density in the prefrontal cortex in schizophrenia and mood disorders: a study from the Stanley Neuropathology Consortium. Schizophr Res. 2004;67:269–75.
58. Kolomeets NS, Uranova NA. Reduced oligodendrocyte density in layer 5 of the prefrontal cortex in schizophrenia. Eur Arch Psychiatry Clin Neurosci. 2019;269:379–86.
59. Foong J, Symms M, Barker G, Maier M, Woermann F, Miller D, et al. Neuropathological abnormalities in schizophrenia: evidence from magnetization transfer imaging. Brain. 2001;124:882–92.
60. Price G, Cercignani M, Chu EM, Barnes TR, Barker GJ, Joyce EM, et al. Brain pathology in first-episode psychosis: magnetization transfer imaging provides additional information to MRI measurements of volume loss. Neuroimage. 2010;49:185–92.
61. Maani R, Yang YH, Kalra S. Voxel-based texture analysis of the brain. PLoS One. 2015;10:e0117759.
62. Maani R, Yang Y-H, Emery D, Kalra S. Cerebral degeneration in amyotrophic lateral sclerosis revealed by 3-dimensional texture analysis. Front. Neurosci. 2016;10:120.
63. Tak K, Lee S, Choi E, Suh SW, Oh DJ, Moon W, et al. Magnetic resonance imaging texture of medial pulvinar in dementia with lewy bodies. Dement Geriatr Cogn Disord. 2020;49:8–15.
64. Sui YV, Bertisch H, Lee H-H, Storey P, Babb JS, Goff DC, et al. Quantitative macromolecular proton fraction mapping reveals altered cortical myelin profile in schizophrenia spectrum disorders. Cereb Cortex Commun. 2021;2:tgab015.
65. Rowley CD, Sehmbi M, Bazin PL, Tardif CL, Minuzzi L, Frey BN, et al. Age-related mapping of intracortical myelin from late adolescence to middle adulthood using T1-weighted MRI. Hum Brain Mapp. 2017;38:3691–703.
66. Edwards LJ, Kirilina E, Mohammadi S, Weiskopf N. Microstructural imaging of human neocortex in vivo. Neuroimage. 2018;182:184–206.
67. Palaniyappan L. Progressive cortical reorganisation: a framework for investigating structural changes in schizophrenia. Neurosci Biobehav Rev. 2017;79:1–13.
68. Abel S, Weiller C, Huber W, Willmes K, Specht K. Therapy-induced brain reorganization patterns in aphasia. Brain. 2015;138:1097–112.
69. Kerr AL, Cheng S-Y, Jones TA. Experience-dependent neural plasticity in the adult damaged brain. J Commun Disord. 2011;44:538–48.
70. Westlye LT, Walhovd KB, Dale AM, Bjørnerud A, Due-Tønnessen P, Engvig A, et al. Differentiating maturational and aging-related changes of the cerebral cortex by use of thickness and signal intensity. Neuroimage. 2010;52:172–85.
71. Palaniyappan L, Das T, Dempster K. The neurobiology of transition to psychosis: clearing the cache. J Psychiatry Neurosci. 2017;42:294–9.
72. Aerts HJ, Velazquez ER, Leijenaar RT, Parmar C, Grossmann P, Carvalho S, et al. Decoding tumour phenotype by noninvasive imaging using a quantitative radiomics approach. Nat Commun. 2014;5:1–9.
73. Van Griethuysen JJ, Fedorov A, Parmar C, Hosny A, Aucoin N, Narayan V, et al. Computational radiomics system to decode the radiographic phenotype. Cancer Res. 2017;77:e104–e107.
74. Moyer CE, Shelton MA, Sweet RA. Dendritic spine alterations in schizophrenia. Neurosci Lett. 2015;601:46–53.

AUTHOR CONTRIBUTIONS

JSK, KWK, and SYM conceived the project. SYM designed the study methodology and wrote the first manuscript with the help of all other authors. HP and WL performed MRI and texture analysis with the help of SL, KWK, and SYM. MK and JSK provided the resources and supervised the project. Review and editing of the first manuscript were performed by MK, JSK, and SYM.

FUNDING

This research was supported by the Basic Science Research Program through the National Research Foundation of Korea (NRF) and the KBRI basic research program through Korea Brain Research Institute, funded by the Ministry of Science & ICT (grant nos. 2019R1C1C1002457, 2020M3E5D9079910, and 21-BR-03-01).

COMPETING INTERESTS

The authors declare no competing interests.

ADDITIONAL INFORMATION

Supplementary information The online version contains supplementary material available at https://doi.org/10.1038/s41380-023-02163-3.

Correspondence and requests for materials should be addressed to Jun Soo Kwon.

Reprints and permission information is available at http://www.nature.com/reprints

Publisher's note Springer Nature remains neutral with regard to jurisdictional claims in published maps and institutional affiliations.